Total Synthesis of a Functional Designer Eukaryotic Chromosome

Narayana Annaluru,[1]* Héloïse Muller,[1,2,3,4]* Leslie A. Mitchell,[2,5] Sivaprakash Ramalingam,[1] Giovanni Stracquadanio,[2,6] Sarah M. Richardson,[6] Jessica S. Dymond,[2,7] Zheng Kuang,[2] Lisa Z. Scheifele,[2,8] Eric M. Cooper,[2] Yizhi Cai,[2,9] Karen Zeller,[2] Neta Agmon,[2,5] Jeffrey S. Han,[10] Michalis Hadjithomas,[11] Jennifer Tullman,[6] Katrina Caravelli,[2,12] Kimberly Cirelli,[1,12] Zheyuan Guo,[1,13] Viktoriya London,[1,13] Apurva Yeluru,[1,13] Sindurathy Murugan,[6] Karthikeyan Kandavelou,[1,14] Nicolas Agier,[15,16] Gilles Fischer,[15,16] Kun Yang,[2,6] J. Andrew Martin,[2,6] Murat Bilgel,[13] Pavlo Bohutski,[13] Kristin M. Boulier,[12] Brian J. Capaldo,[13] Joy Chang,[13] Kristie Charoen,[13] Woo Jin Choi,[13] Peter Deng,[11] James E. DiCarlo,[13] Judy Doong,[13] Jessilyn Dunn,[13] Jason I. Feinberg,[12] Christopher Fernandez,[12] Charlotte E. Floria,[12] David Gladowski,[12] Pasha Hadidi,[13] Isabel Ishizuka,[12] Javaneh Jabbari,[12] Calvin Y. L. Lau,[13] Pablo A. Lee,[13] Sean Li,[13] Denise Lin,[12] Matthias E. Linder,[12] Jonathan Ling,[13] Jaime Liu,[13] Jonathan Liu,[13] Mariya London,[12] Henry Ma,[13] Jessica Mao,[13] Jessica E. McDade,[13] Alexandra McMillan,[12] Aaron M. Moore,[12] Won Chan Oh,[13] Yu Ouyang,[13] Ruchi Patel,[13] Marina Paul,[12] Laura C. Paulsen,[13] Judy Qiu,[13] Alex Rhee,[13] Matthew G. Rubashkin,[13] Ina Y. Soh,[12] Nathaniel E. Sotuyo,[12] Venkatesh Srinivas,[13] Allison Suarez,[13] Andy Wong,[13] Remus Wong,[13] Wei Rose Xie,[12] Yijie Xu,[13] Allen T. Yu,[12] Romain Koszul,[3,4] Joel S. Bader,[2,6] Jef D. Boeke,[2,11,5]† Srinivasan Chandrasegaran[1]†

Rapid advances in DNA synthesis techniques have made it possible to engineer viruses, biochemical pathways and assemble bacterial genomes. Here, we report the synthesis of a functional 272,871–base pair designer eukaryotic chromosome, synIII, which is based on the 316,617–base pair native *Saccharomyces cerevisiae* chromosome III. Changes to synIII include TAG/TAA stop-codon replacements, deletion of subtelomeric regions, introns, transfer RNAs, transposons, and silent mating loci as well as insertion of loxPsym sites to enable genome scrambling. SynIII is functional in *S. cerevisiae*. Scrambling of the chromosome in a heterozygous diploid reveals a large increase in a-mater derivatives resulting from loss of the *MAT*α allele on synIII. The complete design and synthesis of synIII establishes *S. cerevisiae* as the basis for designer eukaryotic genome biology.

Saccharomyces cerevisiae has a genome size of ~12 Mb distributed among 16 chromosomes. The entire genome encodes ~6000 genes, of which ~5000 are individually nonessential (*1*). Which of these nonessential genes are simultaneously dispensable? Although a number of studies have successfully mapped pairwise "synthetic lethal" interactions between gene knockouts, those methods do not scale well to three or more gene combinations because the number of combinations rises exponentially. Our approach to address this question is to produce a synthetic yeast genome with all nonessential genes flanked by loxPsym sites to enable inducible evolution and genome reduction (a process we refer to as SCRaMbLEing) in vivo (*2*, *3*). The availability of a fully synthetic *S. cerevisiae* genome will allow direct testing of evolutionary questions—such as the maximum number of nonessential genes that can be deleted without a catastrophic loss of fitness and the catalog of viable 3-gene, 4-gene, … *n*-gene deletions that survive under a given growth condition—that are not otherwise easily approachable in a systematic unbiased fashion. Engineering and synthesis of viral and bacterial genomes have been reported in the literature (*4*–*11*). An international group of scientists has embarked on constructing a designer eukaryotic genome, Sc2.0 (www.syntheticyeast.org), and here we report the total synthesis of a complete designer yeast chromosome.

Yeast chromosome III, the third smallest in *S. cerevisiae* [316,617 base pairs (bp)], contains the *MAT* locus determining mating type and was the first chromosome sequenced (*12*). We designed synIII according to fitness, genome stability, and genetic flexibility principles developed for the Sc2.0 genome (*2*). The native sequence was edited in silico by using a series of deletion, insertion, and base substitution changes to produce the desired "designer" sequence (Fig. 1, figs. S1 and S2, and supplementary text). The hierarchical wet-laboratory workflow used to construct synIII (Fig. 2) consisted of three major steps: (i) The 750-bp building blocks (BBs) were produced starting from overlapping 60- to 79-mer oligonucleotides and assembled by using standard polymerase chain reaction (PCR) methods (*13*, *14*) by undergraduate students in the Build-A-Genome class at JHU (Fig. 2A) (*15*). The arbitrary naming scheme for the differently sized DNA molecules used in the Sc2.0 project is explained in fig. S3. (ii) The 133 synIIIL (left of the centromere) BBs and 234 synIIIR BBs were assembled into 44 and 83 overlapping DNA minichunks of ~2 to 4 kb, respectively (table S1, Fig. 2B, and fig. S4) (*16*, *17*). (iii) All adjacent minichunks for synIII were designed to overlap one another by one BB to facilitate further assembly in vivo by homologous

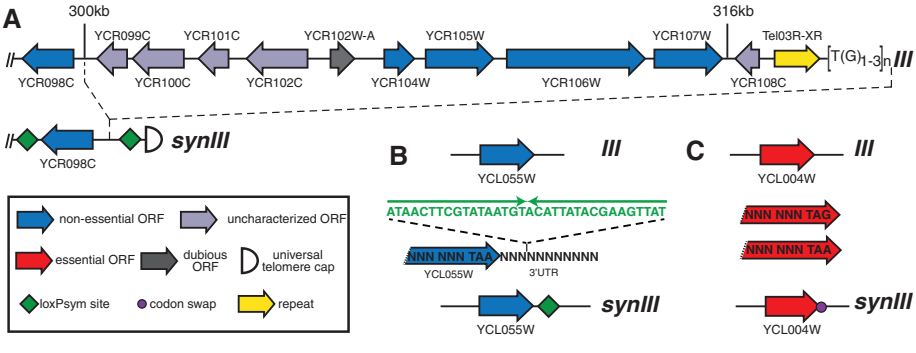

Fig. 1. SynIII design. Representative synIII design segments for loxPsym site insertion (**A** and **B**) and stop codon TAG to TAA editing (**C**) are shown. Green diamonds represent loxPsym sites embedded in the 3′ untranslated region (UTR) of nonessential genes and at several other landmarks. Fuchsia circles indicate synthetic stop codons (TAG recoded to TAA). Complete maps of designed synIII chromosome with common and systematic open reading frame (ORF) names, respectively, are shown in figs. S1 and S2.

[1]Department of Environmental Health Sciences, Johns Hopkins University (JHU) School of Public Health, Baltimore, MD 21205, USA. [2]High Throughput Biology Center, JHU School of Medicine, Baltimore, MD 21205, USA. [3]Group Spatial Regulation of Genomes, Department of Genomes Genetics, Institut Pasteur, F-75015 Paris, France. [4]CNRS, UMR 3525, F-75015 Paris, France. [5]New York University Langone Medical Center, New York, NY 10016, USA. [6]Department of Biomedical Engineering and Institute of Genetic Medicine, Whiting School of Engineering, JHU, Baltimore, MD 21218, USA. [7]Biological Sciences, Research and Exploratory Development Department, JHU Applied Physics Laboratory, Laurel, MD 20723, USA. [8]Department of Biology, Loyola University Maryland, Baltimore, MD 21210, USA. [9]University of Edinburgh, Edinburgh, Scotland, UK. [10]Carnegie Institution of Washington, Baltimore, MD 21218, USA. [11]Department of Biology, JHU, Baltimore, MD 21218, USA. [12]Krieger School of Arts and Sciences, JHU, Baltimore, MD 21218, USA. [13]Whiting School of Engineering, JHU, Baltimore, MD 21218, USA. [14]Pondicherry Biotech Private Limited, Pillaichavady, Puducherry 605014, India. [15]Sorbonne Universités, Université Pierre et Marie Curie, Univ Paris 06, UMR 7238, Génomique des Microorganismes, F-75005 Paris, France. [16]CNRS, UMR7238, Génomique des Microorganismes, F-75005 Paris, France.

*These authors contributed equally to this work.
†Corresponding author. E-mail: jef.boeke@nyumc.org (J.D.B.); schandra@jhsph.edu (S.C.)

recombination in yeast (*18*, *19*). By using an average of 12 minichunks and alternating selectable markers in each experiment, we systematically replaced the native sequence of *S. cerevisiae* III with its synIII counterpart in 11 successive rounds of transformation (Fig. 2C and table S2) (*20*, *21*).

Genome Comparisons

PCRTag analysis (*2*) revealed the presence of synIII synthetic PCRTags and absence of native PCRTags (Fig. 3A; see supplementary text and figs. S5 to S7 for the complete set of PCRTag analyses). The smaller size of synIII and intermediates in its full synthesis as compared with the native yeast chromosome was demonstrated by pulsed-field gel electrophoresis (Fig. 3B and fig. S8) (*22*). Analysis of the intermediate strains revealed that the starting strain had some unexpected rearrangements in at least two chromosomes and that an additional rearrangement occurred during the assembly process; these did not affect synIII (fig. S8). These abnormalities were eliminated through back-crossing the synIIIL intermediate strain to strain BY4742 (table S3), yielding a *MATα* strain with an electrophoretic karyotype perfectly matching BY4742 but for the expected altered length III (compare lane 97 to 97* in fig. S8). Southern blot analyses using arm-specific radiolabeled probes further verified and validated the structure of the left- and right-arm telomere ends of synIII, which had been specified by the universal telomere cap (UTC) sequence (fig. S9). Restriction fragment sizes on Southern blots are compatible with the deletion of *HML*, *HMR*, and much of each subtelomere (fig. S9). This was further confirmed by complete genome sequencing of the synIII strain.

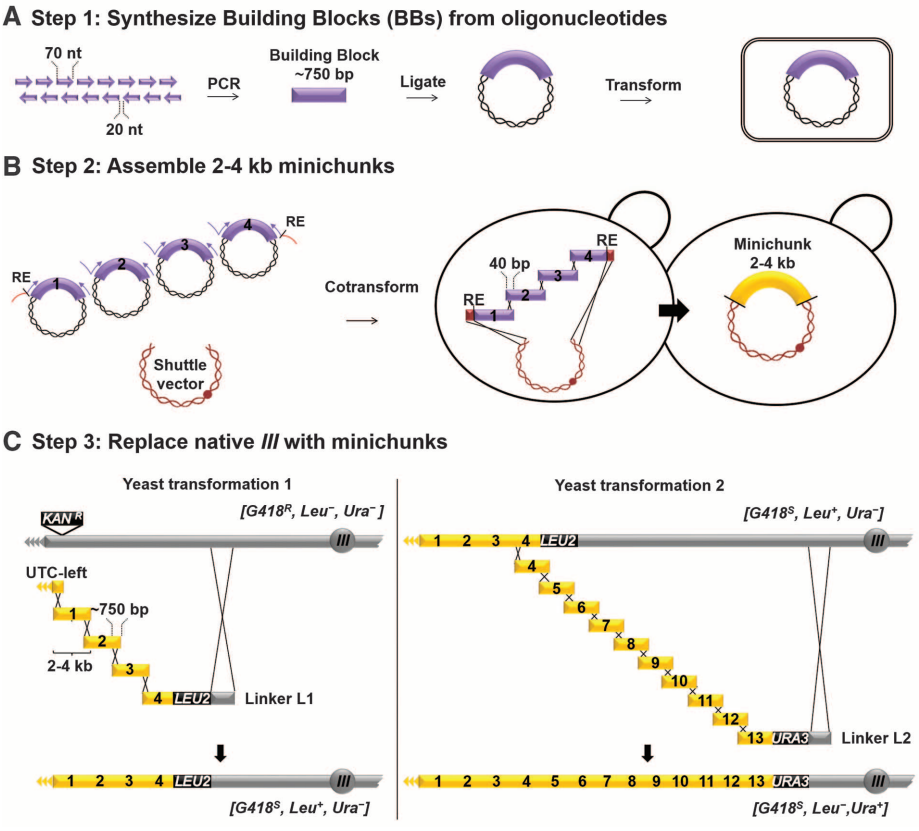

Fig. 2. SynIII construction. (**A**) BB synthesis. JHU students in the Build-A-Genome course synthesized 750-bp BBs (purple) from oligonucleotides. nt, nucleotides. (**B**) Assembly of minichunks. Two- to 4-kb minichunks (yellow) were assembled by homologous recombination in *S. cerevisiae* (table S1). Adjacent minichunks were designed to encode overlap of one BB to facilitate downstream assembly steps. Minichunks were flanked by a rare cutting restriction enzyme (RE) site, *Xma*I or *Not*I. (**C**) Direct replacement of native yeast chromosome III with pools of synthetic minichunks. Eleven iterative one-step assemblies and replacements of native genomic segments of yeast chromosome III were carried out by using pools of overlapping synthetic DNA minichunks (table S2), encoding alternating genetic markers (*LEU2* or *URA3*), which enabled complete replacement of native III with synIII in yeast.

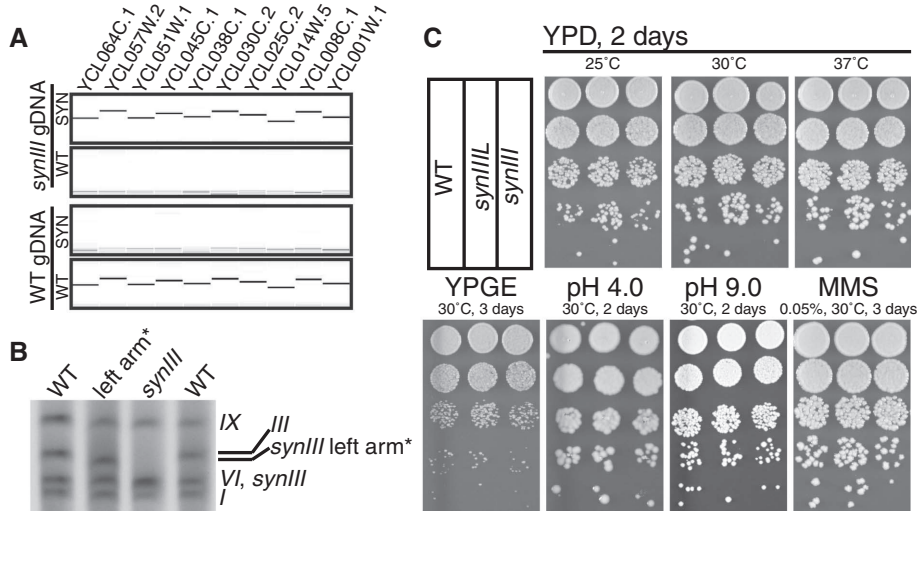

Fig. 3. Characterization and testing of synIII strain. (**A**) PCRTag analysis (one PCRTag per ~10 kb) of the left arm of synIII and WT yeast (BY4742) DNA is shown. Analysis of the complete set of PCRTags is shown in figs. S4 to S6. (**B**) Karyotypic analysis of synIII and synIIIL strains by pulsed-field gel electrophoresis revealed the size reduction of synIII and synIIIL compared with native III. Yeast chromosome numbers are indicated on the right side. SynIII (272,871 bp) and native chromosome VI (270,148 bp) comigrate in the gel. A karyotypic analysis of synIII and all intermediate strains is shown in fig. S8. (**C**) SynIII and synIIIL phenotyping on various types of media. Tenfold serial dilutions of saturated cultures of WT (BY4742), synIIIL, and synIII strains were plated on the indicated media and temperatures. YPD, yeast extract peptone dextrose; YPGE, yeast extract peptone glycerol ethanol; MMS, methyl methanosulfate. A complete set of synIII and synIIIL phenotyping under various conditions is shown in fig. S11.

DNA sequencing of the synIII strain genome revealed sequence differences at 10 sites in synIII compared with our designed sequence (table S4). Nine of the changes are base substitutions or 1-bp insertions or deletions (indels). Three of the nine mutations correspond to preexisting but apparently innocuous mutations in the minichunks and BBs. Of the remainder, two correspond to the wild-type (WT) base at this position and thus may simply reflect inheritance of WT sequence. Because PCRTag analysis (table S5) was the method used to validate transformants during the 11 intermediate construction steps, the recombination events involved are patchy transformants, with tiny patches of native DNA instead of synthetic sequence that would have been missed during the PCRTag analysis. The remaining four mutations, which must have originated during the integration process, all occur in regions of overlap in the synIII minichunks, suggesting that the homologous recombination process may be somewhat error-prone relative to baseline error rates (*23*). The tenth change is the absence of an expected loxPsym site.

To check for negative effects of modifications on fitness of synIII-containing strains from the WT (BY4742), we examined colony size, growth curves, and morphology under various conditions. A growth curve analysis established that synIII and the isogenic native strain had no detectable fitness difference (fig. S10). The strains were also indistinguishable from each other on colony-size tests (Fig. 3C), indicating that defects in fitness attributable to the synIIIL intermediate or synIII are very modest, with only 1 condition out of 21 (high sorbitol) showing a subtle fitness defect for synIII (fig. S11). Cell morphology of all intermediate strains was similar to that of WT (fig. S12) except that, during replacement round R3 (giving rise to strain 219 kb-synIII), a very low frequency (~1% of cells) of morphologically abnormal buds were observed (fig. S12). We performed transcript profiling to identify possible changes in gene expression across synIII or genome-wide resulting from synonymous substitutions, introduction of loxPsym sites, and other changes. Although 10 loci are differentially expressed at genome-wide significance ($P < 7.4 \times 10^{-6}$ for 5% family-wise error rate based on 6756 loci with at least one mapped read and also corresponding to 1% false discovery rate), eight of these correspond to loci intentionally deleted from synIII. The remaining two loci are *HSP30* on synIII, ~16-fold down, and *PCL1* on native chromosome *XIV*, ~16-fold up (fig. S13).

The inclusion of hundreds of designed changes in the synthetic chromosome, including the removal of 11 transfer RNA (tRNA) genes said to be important sites of cohesin loading, might result in subtle or overt destabilizing effects on the synthetic chromosome; alternatively, removal of repetitive DNA sequences might increase stability by reducing the likelihood of "ectopic" recombination events involving two different repeat copies. Because of the 98 loxPsym sites added to synIII (and all the other changes), it was important to evaluate the genome integrity and the loss rate of the chromosome in the absence of Cre expression. PCRTag analysis revealed that synIII is stable over 125 mitotic generations in 30 independent lineages (Fig. 4A). To evaluate the loss rate of synIII, we used the a-like faker assay in which *MAT*α cells carrying synIII were monitored for acquiring the ability to mate as *MAT***a** cells, a consequence of losing chromosome III (*24*). Despite the extensive chromosome engineering, the frequency of *MAT*α/synIII loss was not significantly different from that of the WT control (Fig. 4B).

It is not known whether cohesin accumulation at a tRNA gene region directly depends on the presence of the tRNA gene, nor is its effect on chromosome stability clear. We compared the map of cohesin binding sites on native chromosome III and synIII by using chromatin immunoprecipitation sequence (ChIP-seq) analysis (fig. S14). The overall cohesin binding pattern is similar between the two chromosomes. However, at three tRNA genes that show a prominent peak in the native chromosome, that peak is reduced or in one case [the glutamine tRNA gene tQ(UUG)C] completely absent from synIII (fig. S14). Thus, we conclude that tRNA genes and their documented interactions with both cohesin and condensin (*25*, *26*) are dispensable for high levels of chromosome stability. We also compared the replication dynamics of synIII and native III (supplementary text, table S9, and fig. S15) and saw few dramatic changes in dynamics in spite of several autonomously replicating sequences having been deleted.

SCRaMbLEing in haploid strains containing chromosome synIII leads to lethality via essential gene loss (fig. S16). We looked for more subtle effects of SCRaMbLE in a heterozygous *MAT***a**/α (mating incompetent) diploid strain with a synthetic *MAT*α chromosome and a native *MAT***a** chromosome synIII/III; (fig. S17). We introduced the Cre-EBD plasmid into such strains, as well as into

A

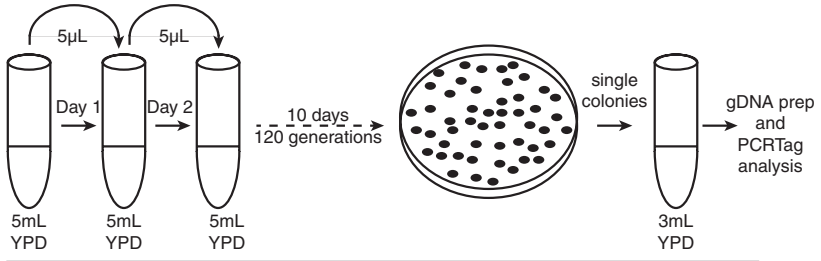

Number of Generations	Number of Strains	Non-essential segments	Deletions Observed	Frequency
~125	30	58	0	$< 4.6 \times 10^{-6}$

B

Strain	Total number cells plated	Colonies on SD	Average loss rate
synIII	$\sim 1.6 \times 10^{9}$	1013	$6.7 \times 10^{-7} \pm 3.9 \times 10^{-7}$
WT	$\sim 1.9 \times 10^{9}$	830	$4.6 \times 10^{-7} \pm 1.3 \times 10^{-7}$

C

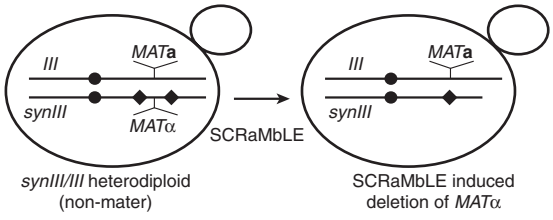

Strain	Frequency (%)	
	a-mater	α-mater
synIII/III	45	0
III/III	0	0

Fig. 4. Genomic stability of the synIII strain. (**A**) PCRTag analysis of synIII strain after ~125 generations. We assayed for the loss of 58 different segments lacking essential genes in the absence of SCRaMbLEing; no losses were observed after over 200,000 segment-generations analyzed; reported frequency is a maximum estimate of segment loss frequency per generation. gDNA, genomic DNA. (**B**) Evaluation of the loss rate of synIII chromosome using a-like faker assay. No significant change in the loss frequency was observed, although the absolute loss rate value is modestly higher in synIII. SD, standard dextrose. (**C**) SCRaMbLE leads to a gain of mating type a behavior in synIII heterozygous diploids. Frequencies are of a-mater and α-mater colonies post-SCRaMbLE (induction with estradiol) in synIII/III and III/III strains. A complete SCRaMbLE analysis is shown in fig. S18. Diamonds represent loxPsym sites, and circles indicate centromeres.

WT *MAT*a/α diploids (III/III), and very briefly induced with estradiol. In spite of the minimal level of SCRaMbLEing induced, we observed a massive increase in the frequency of a-mater derivatives in the native III/synIII heterozygous strains (Fig. 4C and fig. S18). Such a-mater derivatives can arise from the loss of the *MAT*α locus, because such *MAT*-less strains express a-specific genes. PCRTag mapping of several such derivatives showed that these variants had indeed lost different sections of synIII, all of which included the *MAT* locus (fig. S18).

The total synthesis of the synIII chromosome represents a major step toward the design and complete synthesis of a novel eukaryotic genome structure using the model *S. cerevisiae* as the basis for a synthetic designer genome, Sc2.0. The many changes made to synIII, including intron deletion, tRNA gene removal, and loxPsym sites and PCRTags introduction, do not appear to significantly decrease the fitness or alter the transcriptome or the replication timing of the synIII strain, supporting the very pliable nature of the yeast genome and potentially allowing for much more aggressively redesigned future genome versions. Sc2.0 represents just one of myriad possible arbitrary genome designs, and we anticipate that synthetic chromosome design will become a new means of posing specific evolutionary and mechanistic questions about genome structure and function. Rapid advances in synthetic biology coupled with ever decreasing costs of DNA synthesis suggest that it will soon become feasible to engineer new eukaryotic genomes, including plant and animal genomes, with synthetic chromosomes encoding desired functions and phenotypic properties based on specific design principles.

References and Notes

1. A. Goffeau *et al*., *Science* **274**, 546–567 (1996).
2. J. S. Dymond *et al*., *Nature* **477**, 471–476 (2011).
3. J. Dymond, J. Boeke, *Bioeng. Bugs* **3**, 168–171 (2012).
4. J. Cello, A. V. Paul, E. Wimmer, *Science* **297**, 1016–1018 (2002).
5. L. Y. Chan, S. Kosuri, D. Endy, *Mol. Syst. Biol.* **1**, 0018 (2005).
6. G. Pósfai *et al*., *Science* **312**, 1044–1046 (2006).
7. D. G. Gibson *et al*., *Science* **319**, 1215–1220 (2008).
8. C. Lartigue *et al*., *Science* **317**, 632–638 (2007).
9. H. H. Wang *et al*., *Nature* **460**, 894–898 (2009).
10. D. G. Gibson *et al*., *Science* **329**, 52–56 (2010).
11. F. J. Isaacs *et al*., *Science* **333**, 348–353 (2011).
12. S. G. Oliver *et al.*, *Nature* **357**, 38–46 (1992).
13. S. M. Richardson, S. J. Wheelan, R. M. Yarrington, J. D. Boeke, *Genome Res.* **16**, 550–556 (2006).
14. W. P. Stemmer, A. Crameri, K. D. Ha, T. M. Brennan, H. L. Heyneker, *Gene* **164**, 49–53 (1995).
15. J. S. Dymond *et al*., *Genetics* **181**, 13–21 (2009).
16. N. Annaluru *et al*., *Methods Mol. Biol.* **852**, 77–95 (2012).
17. D. G. Gibson *et al*., *Nat. Methods* **6**, 343–345 (2009).
18. H. Ma, S. Kunes, P. J. Schatz, D. Botstein, *Gene* **58**, 201–216 (1987).
19. V. Larionov *et al*., *Proc. Natl. Acad. Sci. U.S.A.* **93**, 491–496 (1996).
20. D. G. Gibson *et al*., *Proc. Natl. Acad. Sci. U.S.A.* **105**, 20404–20409 (2008).
21. H. Muller *et al*., *Methods Mol. Biol.* **852**, 133–150 (2012).
22. D. C. Schwartz, C. R. Cantor, *Cell* **37**, 67–75 (1984).
23. M. Lynch *et al*., *Proc. Natl. Acad. Sci. U.S.A.* **105**, 9272–9277 (2008).
24. K. W. Yuen *et al*., *Proc. Natl. Acad. Sci. U.S.A.* **104**, 3925–3930 (2007).
25. C. D'Ambrosio *et al*., *Genes Dev.* **22**, 2215–2227 (2008).
26. A. Lengronne *et al*., *Nature* **430**, 573–578 (2004).

Acknowledgments: This work was supported by grants from NSF (MCB 0718846) to J.D.B., J.S.B., and S.C. and from Microsoft to J.S.B. S.M. and S.C were supported by a grant from NIH (GM077291 to S.C.); H. Muller, by a fellowship from Fondation pour la Recherche Médicale and a Pasteur-Roux fellowship; S.R., by an Exploratory Research Grant from the Maryland Stem Cell Research Fund; L.A.M., by a fellowship from the National Sciences and Engineering Research Council of Canada; S.M.R., by a fellowship from the U.S. Department of Energy; and J.S.D., by a fellowship from JHU Applied Physics Laboratory. We thank D. Gibson for helpful suggestions regarding the isothermal assembly reaction, E. Louis and D. Gottschling for advice on synthetic telomere design, and L. Teytelman and J. Rine for advice on silent cassette DNA. The synIII sequences have been deposited at GenBank with accession numbers KJ463385 (the as-designed reference sequence version 3.3_41) and KC880027 (the actual physical sequence in strain HMSY011, sequence version 3.3_42). The authors declare no competing financial interests. Requests for materials should be addressed to J.D.B. (boekej01@nyumc.org). We dedicate this publication to the memory of Har Gobind Khorana, who synthesized the first yeast tRNA gene. N. Annaluru, H. Muller, J.S.B., J.D.B., and S.C. designed experiments. J.D.B. and S.M.R. designed synIII. N. Annaluru, H.M., L.A.M., S.R., G.S., S.M.R., J.S.D., Z.K., Y.C., Z.G., V.L., S.M., K.K., N. Agmon, G.F., and S.C. performed experiments. N. Annaluru, H.M., G.S., R.K., J.D.B., and S.C. analyzed data. N. Annaluru, H.M., J.D.B., and S.C. wrote the manuscript. JHU Build-A-Genome course students (K. Caravelli, K. Cirelli, Z.G., V.L., A.Y., M.B., P.B., K.M.B., B.J.C., J.C., K. Charoen, W.J.C., P.D., J.E.D., J. Doong, J. Dunn, J.I.F., C.F., C.E.F., D.G., P.H., I.I., J.J., C.Y.L.L., P.A.L., S.L., D.L., M.E.L., J. Ling, Jaime Liu, Jonathan Liu, M.L., H.Ma, J.M., J.E.M., A.M., A.M.M., W.C.O., Y.O., R.P., M.P., L.C.P., J.Q., A.R., M.G.R., I.Y.S., N.E.S., V.S., A.S., A.W., R.W., W.R.X., Y.X., A.T.Y.) synthesized most of the building blocks for synIII; H. Muller, G.S., S.M.R., J.S.D., L.Z.S., E.M.C., Y.C., K.Z., J.S.H., M.H., J.T. and J.D.B. taught the Build-A-Genome course. S.C. led the effort on the construction and assembly of synIII.

Supplementary Materials

www.sciencemag.org/content/344/6179/55/suppl/DC1
Materials and Methods
Supplementary Text
Fig. S1
Table S1
References (*27*–*48*)

3 December 2013; accepted 6 March 2014
Published online 27 March 2014;
10.1126/science.1249252

Structure of a Class C GPCR Metabotropic Glutamate Receptor 1 Bound to an Allosteric Modulator

Huixian Wu,[1]* Chong Wang,[1]* Karen J. Gregory,[2,3] Gye Won Han,[1] Hyekyung P. Cho,[2] Yan Xia,[4] Colleen M. Niswender,[2] Vsevolod Katritch,[1] Jens Meiler,[4] Vadim Cherezov,[1] P. Jeffrey Conn,[2] Raymond C. Stevens[1]†

The excitatory neurotransmitter glutamate induces modulatory actions via the metabotropic glutamate receptors (mGlus), which are class C G protein–coupled receptors (GPCRs). We determined the structure of the human $mGlu_1$ receptor seven-transmembrane (7TM) domain bound to a negative allosteric modulator, FITM, at a resolution of 2.8 angstroms. The modulator binding site partially overlaps with the orthosteric binding sites of class A GPCRs but is more restricted than most other GPCRs. We observed a parallel 7TM dimer mediated by cholesterols, which suggests that signaling initiated by glutamate's interaction with the extracellular domain might be mediated via 7TM interactions within the full-length receptor dimer. A combination of crystallography, structure-activity relationships, mutagenesis, and full-length dimer modeling provides insights about the allosteric modulation and activation mechanism of class C GPCRs.

The human G protein–coupled receptor (GPCR) superfamily comprises more than 800 seven-transmembrane (7TM) receptors that can be divided into four classes according to their sequence homology: class A, B, C, and F (Frizzled) (*1*). Class C GPCRs play important roles in many physiological processes such as synaptic transmission, taste sensation, and calcium homeostasis; they include metabotropic glutamate receptors (mGlus), γ-aminobutyric acid B ($GABA_B$) receptors, calcium-sensing (CaS) receptors, and taste 1 (TAS1) receptors, as well as a few orphan receptors. A distinguishing feature of class C GPCRs is constitutive homo- or heterodimerization mediated by a large N-terminal extracellular domain (ECD) (Fig. 1A). The ECDs within homodimeric receptors (mGlu and CaS) are cross-linked via an intermolecular disulfide bond. The heterodimeric receptors ($GABA_B$ and TAS1) are not covalently linked, but their heterodimerization is required for trafficking to the cell surface and signaling (*2*). The ECD of class C

[1]Department of Integrative Structural and Computational Biology, The Scripps Research Institute, 10550 North Torrey Pines Road, La Jolla, CA 92037, USA. [2]Department of Pharmacology and Vanderbilt Center for Neuroscience Drug Discovery, Vanderbilt University Medical Center, Nashville, TN 37232, USA. [3]Drug Discovery Biology, Monash Institute of Pharmaceutical Sciences, Monash University, Parkville, Victoria, Australia. [4]Center for Structural Biology and Department of Chemistry and Institute for Chemical Biology, Vanderbilt University Medical Center, Nashville, TN 37232, USA.

*These authors contributed equally to this work.
†Corresponding author. E-mail: stevens@scripps.edu